

Efficient Discovery of Potent Anti-HIV Agents Targeting the Tyr181Cys Variant of HIV Reverse Transcriptase

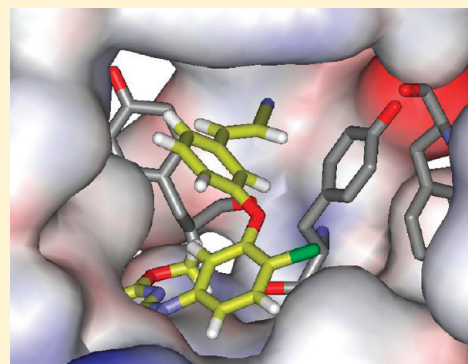
William L. Jorgensen,^{*,†} Mariela Bollini,[†] Vinay V. Thakur,[†] Robert A. Domaoal,[‡] Krasimir A. Spasov,[‡] and Karen S. Anderson^{*,‡}

[†]Department of Chemistry, Yale University, New Haven, Connecticut 06520-8107, United States

[‡]Department of Pharmacology, Yale University School of Medicine, New Haven, Connecticut 06520-8066, United States

S Supporting Information

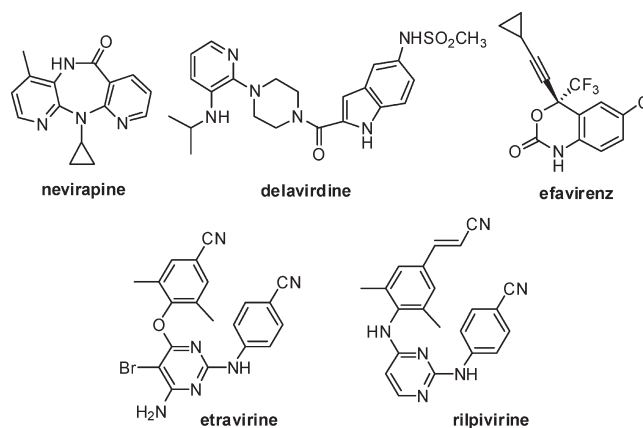
ABSTRACT: Non-nucleoside reverse transcriptase inhibitors (NNRTIs) that interfere with the replication of human immunodeficiency virus (HIV) are being pursued with guidance from molecular modeling including free-energy perturbation (FEP) calculations for protein–inhibitor binding affinities. The previously reported pyrimidinylphenylamine **1** and its chloro analogue **2** are potent anti-HIV agents; they inhibit replication of wild-type HIV-1 in infected human T-cells with EC₅₀ values of 2 and 10 nM, respectively. However, they show no activity against viral strains containing the Tyr181Cys (Y181C) mutation in HIV-RT. Modeling indicates that the problem is likely associated with extensive interaction between the dimethylallyloxy substituent and Tyr181. As an alternative, a phenoxy group is computed to be oriented in a manner diminishing the contact with Tyr181. However, this replacement leads to a roughly 1000-fold loss of activity for **3** (2.5 μM). The present report details the efficient, computationally driven evolution of **3** to novel NNRTIs with sub-10 nM potency toward both wild-type HIV-1 and Y181C-containing variants. The critical contributors were FEP substituent scans for the phenoxy and pyrimidine rings and recognition of potential benefits of addition of a cyanovinyl group to the phenoxy ring.



INTRODUCTION

Non-nucleoside reverse transcriptase inhibitors (NNRTIs) that interfere with the replication of human immunodeficiency virus (HIV) are an important component of highly active antiretroviral therapy (HAART).¹ They are known to function by binding to an allosteric pocket in the vicinity of the RT's polymerase active site.² Though there are five FDA-approved drugs in the class (nevirapine, delavirdine, efavirenz, etravirine, and rilpivirine), alternatives are needed for first-line therapy owing to issues of safety, resistance, and ease of administration.^{1,3} Common side effects associated with the currently approved drugs include severe skin reactions, liver toxicity, and sleep disorders. In view of the rapid mutation of the virus, drug resistance is problematic, and the NNRTIs are given in combination therapies. Though the class has demonstrated significant utility and promise, further improvements are undoubtedly possible. There is also a need to be positioned to respond to the emergence of pan-resistant viral variants and unknown effects of long-term treatment.⁴

In our own pursuit of new NNRTIs, we have simultaneously sought improved computational methods of general utility to streamline the discovery process.⁵ The basic goal is to minimize the number of compounds that have to be synthesized and assayed to yield a drug candidate. Our computational approach is multifaceted, including virtual screening, *de novo* design, prediction of pharmacological properties and metabolites, and lead



optimization guided by molecular modeling including free-energy perturbation (FEP) calculations.⁵ Though success has been demonstrated in the discovery and optimization of NNRTIs in several structural series,⁶ improvement in the performance against HIV variants with clinically relevant RT mutations is desired. Salient examples are provided by **1** and **2**. They yield inhibitory activity (EC₅₀) values of 2 and 10 nM,^{6b}

Received: June 23, 2011

Published: August 19, 2011

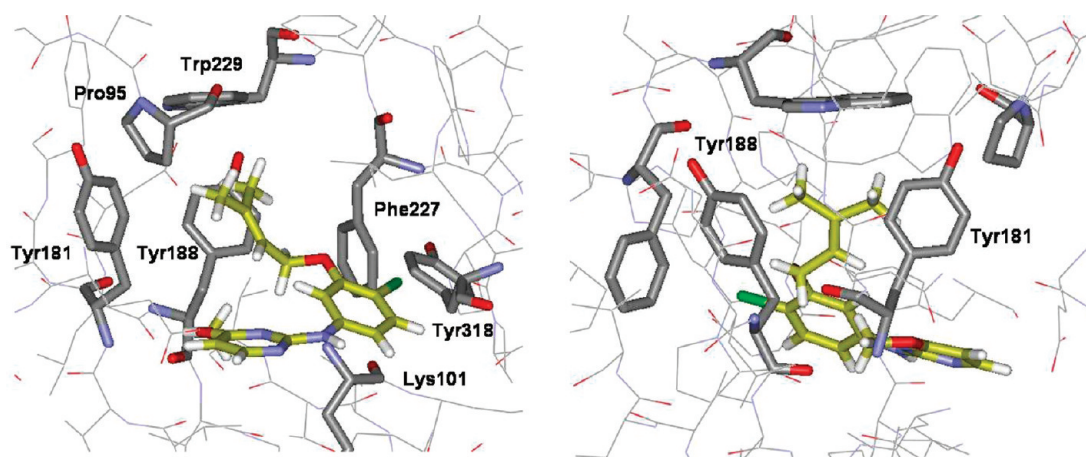


Figure 1. Two orientations of NNRTI **2** bound to WT HIV-RT, as created using BOMB⁵ and optimized using MCPRO.⁸ The full model contains ca. 175 protein residues and the inhibitor. Carbon atoms of the NNRTI are colored gold. The image on the right is rotated 90° from the one on the left.

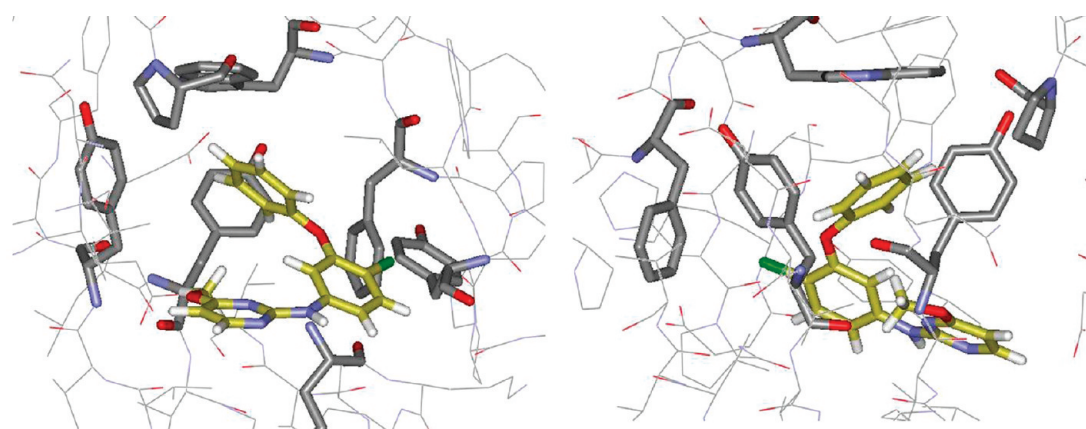
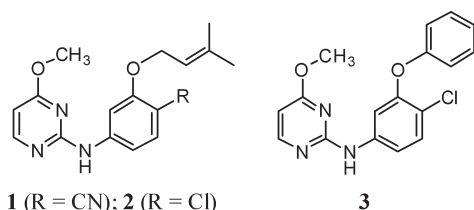


Figure 2. The same views as in Figure 1, but with NNRTI **3** bound to HIV-RT. Modeling suggested substitutions at the 3- and 5-positions in the phenoxy ring with possible passage of a substituent between Tyr181 and Tyr188 or toward Pro95.

respectively, for inhibition of replication of wild-type (WT) HIV-1 in infected human T-cells. The activity for **1** is essentially the same as for efavirenz and etravirine in this assay and far greater than for nevirapine (110 nM). However, similar to nevirapine, **1** and **2** show no activity against virus encoding the Tyr181Cys (Y181C) mutation in the RT enzyme. This mutation often arises early in patients treated with NNRTIs.¹ Most first-generation NNRTIs including nevirapine and delavirdine do not have useful activity toward Y181C containing variants, while efavirenz, etravirine, and rilpivirine retain 1–10 nM potency.⁷



A computed structure for **2** bound to WT HIV-RT is illustrated in Figure 1. Confidence in the structure comes from past experience with complexes for other NNRTIs including numerous crystal structures.^{2–6} Key features are the placement of the *O*-dimethylallyl (ODMA) group in the π -box formed by Tyr181, Tyr188, Phe227, and Trp229, and the hydrogen bond

between the oxygen of Lys101 and the amino group of **2**. The expectation has been that the inactivity toward the Y181C variant stems largely from loss of the favorable contact between Tyr181 and the ODMA group. Thus, ca. 15 alternatives to the ODMA group were tested, but they all led to much less potent or inactive inhibitors for replication of the WT virus.^{6b,c}

Nevertheless, in model building with the molecular growing program BOMB,⁵ the phenoxy-substituted analogue **3** is intriguing. It appears to deemphasize the interaction with Tyr181 in favor of an edge-to-face interaction between the phenyl rings of the phenoxy group and Tyr188, as illustrated in Figure 2. The problem is that the EC₅₀ value for **3** deteriorates roughly 1000-fold to 2.5 μ M.^{6c} However, with experience gained with FEP-guided lead optimization,⁶ a challenge deemed worth pursuing was possible optimization of the substituents in the phenoxy and pyrimidine rings of **3** to seek analogues that would be very potent, e.g., with ca. 10 nM EC₅₀ values, against both WT HIV-1 and variants containing the Y181C RT mutation.

COMPUTATIONAL DETAILS

The key computations were conjugate gradient energy minimizations for protein–inhibitor complexes and FEP calculations to estimate differences in free energies of binding for series of inhibitors.

The energetics for the systems were represented by classical force fields: the OPLS-AA force field for the protein, OPLS/CMA for the inhibitors, and TIP4P for water molecules.⁸ The conjugate gradient optimizations use a dielectric constant of 2 to dampen the Coulombic interactions and 9-Å residue-based cutoffs. The configurational sampling for the FEP calculations was performed via Monte Carlo (MC) statistical mechanics simulations. In the MC/FEP calculations, small changes are made to convert one inhibitor to another, both unbound in water and bound to the protein; the difference in the two resultant free energy changes gives the relative free energy of binding, $\Delta\Delta G_b$.^{9,10} Standard protocols were followed.^{5,6} Briefly, all initial structures were generated with the molecule growing program BOMB starting from the 1s9e PDB file;¹¹ the ligand was removed and replaced by cores such as aniline that are used by BOMB to grow the desired inhibitors in the binding site.⁵ For the Y181C variant, the 1s9e structure was also used as the starting point, and the tyrosine was manually modified to cysteine. A reduced model of the protein was utilized that consisted of the ca. 175 amino acid residues closest to the NNRTI binding site; a few remote side chains were neutralized so that there was no net charge for the protein. The energy minimizations and MC/FEP calculations were executed with MCPRO.⁸ For the MC simulations, 1250 and 2000 water molecules in 25-Å caps were included for the complexes and unbound inhibitors, respectively. All degrees of freedom were sampled for the inhibitors, while the TIP4P water molecules only translated and rotated, as usual. Bond angles and dihedral angles for protein side chains were also sampled, while the backbone was kept fixed after conjugate gradient relaxation.

The FEP calculations typically utilized 11 windows of simple overlap sampling for each modification of a non-hydrogen atom, e.g., $\text{CH}_3 \rightarrow \text{H}$ or $\text{Cl} \rightarrow \text{F}$.^{10b,12} For the simulations of the protein–inhibitor complexes, each window covered at least 15 million (M) configurations of equilibration and 10M configurations of averaging. A window refers to

a MC simulation at one point along the mutation coordinate λ , which interconverts two inhibitors as λ goes from 0 to 1; two free-energy changes are computed at each window, corresponding to forward and backward increments. The spacing between windows, $\Delta\lambda$, is 0.1. The ligand and side chains within ca. 10 Å of the ligand were fully flexible, while the protein backbone was kept fixed during the MC runs. For the perturbations of the unbound inhibitors in water, equilibration covered 30M configurations for the first window and 15M for subsequent ones, while the averaging periods were extended to 40M configurations. With current 3.0-GHz processors (Intel Q9650 Core2), the FEP calculations take approximately 4 days for the complex and 1 day for the inhibitor alone in water on a single processor. It is easy to run the FEP windows simultaneously such that, with 12 processors, one $\Delta\Delta G_b$ result can be obtained in 1 day.

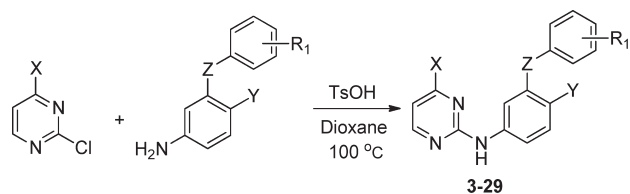
All MC simulations were run at 298 K. The reported uncertainties ($\pm 1\sigma$) for the free energy changes were obtained from the fluctuation in separate averages over batches of 2M configurations.¹³ Equation 1 is used, where m is the number of batches, θ_i is the average of property θ for the i th batch, and $\langle\theta\rangle$ is the overall average for θ . Convergence is also checked through the hystereses in closed FEP cycles, as illustrated below.

$$\sigma^2 = \sum_i^m (\theta_i - \langle\theta\rangle)^2 / m(m-1) \quad (1)$$

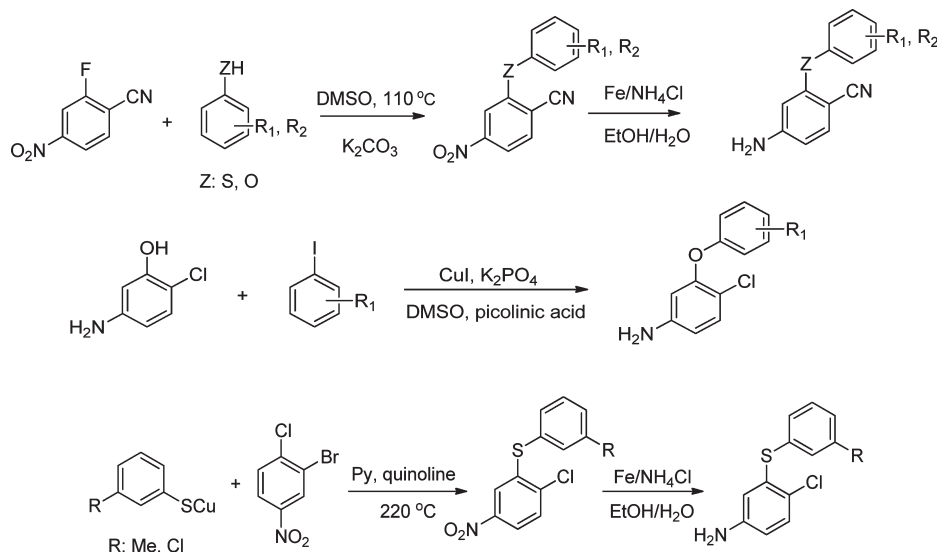
EXPERIMENTAL DETAILS

The syntheses of analogues of **3** and the corresponding 1,3,5-triazine benefited from previously described procedures.^{6b,c} Typically, the desired compounds arose from $\text{S}_\text{N}\text{Ar}$ reaction of phenoxy or thiophenoxy anilines with heteroaryl chlorides (Scheme 1). The required anilines were also mostly prepared by $\text{S}_\text{N}\text{Ar}$ chemistry from substituted phenols or thiophenols and 2-fluoro-4-nitrobenzonitrile (Scheme 2).¹⁴ However, when Y was chlorine, substitution of the chlorine was circumvented by copper-catalyzed selective *O*-arylation of 3-aminophenols,¹⁵ while the corresponding thioethers were prepared using cuprous thiophenolates (Scheme 2).¹⁶ Subsequently, when 3-cyanovinyl-substituted phenols were required, Heck coupling of aryl iodides with acrylonitrile using $\text{PdCl}_2(\text{PPh}_3)_2$ as catalyst was effective (Scheme 3). This reaction afforded separable mixtures of *E*:*Z* (80:20) stereoisomers in 80–90% yield.¹⁷ Finally, some of the most potent compounds were cyclopropyl-triazine analogues, which were prepared according to Scheme 4.

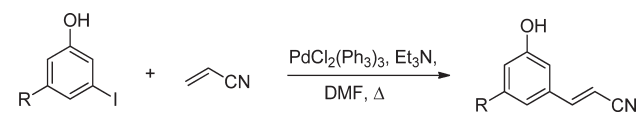
Scheme 1. General Procedure for Synthesis of Heteroaryl-aminodiphenyl Ethers



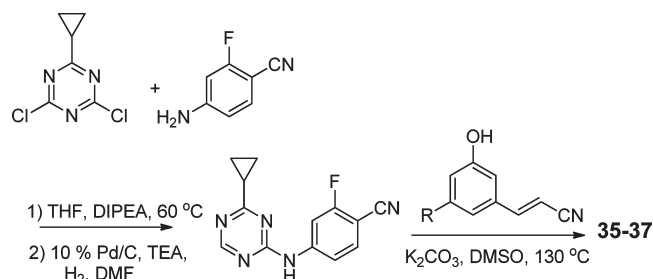
Scheme 2. General Procedures for Syntheses of Diphenyl Ethers and Thioethers



Scheme 3. Synthesis of Cyanovinyl-Substituted Phenols



Scheme 4. Synthesis of Cyclopropyltriazine Analogues



Reaction between 2,4-dichloro-6-cyclopropyl-1,3,5-triazine and 4-amino-2-fluorobenzonitrile gave the corresponding intermediate, which was dechlorinated and coupled with 3-cyanovinyl-substituted phenols to yield the target compounds. Complete synthetic details are provided in the Supporting Information. The identity of all assayed compounds was confirmed by ^1H and ^{13}C NMR and high-resolution mass spectrometry; purity was normally >95% as judged by high-performance liquid chromatography.

For the biology, the primary assay determined activities against the wild-type IIIB strain of HIV-1¹⁸ using MT-2 human T-cells¹⁹ at a multiplicity of infection of 0.1; EC_{50} values are obtained as the dose required for 50% protection of the infected cells using the MTT colorimetric method. The cytotoxicity (CC_{50}) for inhibition of MT-2 cell growth in the absence of virus by 50% is obtained simultaneously.^{20,21} Analogous assays were performed using a variant HIV strain that encodes the Tyr181Cys (Y181C) mutation of HIV-RT.²² All assays were run in triplicate at inhibitor concentrations up to 100 μM .

RESULTS

Alternative Conformers. The initially predicted structure of the parent 3 bound to RT is illustrated in Figure 2; it was built using

BOMB and then subjected to conjugate gradient optimization using MCPRO. An alternative conformer for the bound ligand was also found as illustrated in Figure 3. The conformer from Figure 2 has the faces of the two phenyl rings roughly perpendicular, while the alternative is more reminiscent of a clamshell. The phenoxy groups are nearly orthogonal in the two complexes, though in both cases the interaction with Tyr181 appears to be reduced from what occurs with the ODMA group (Figure 1). The computed protein–ligand interaction energies from optimization of the two complexes are essentially identical at -65.5 kcal/mol. The conformational energetics were then investigated to try to better assess the relative likelihood of the two alternatives.

The optimized dihedral angles for the C–C–O–C–C fragment are 16° and 43° for the perpendicular conformer and 71° and 37° for the clamshell in the complexes. For isolated diphenyl ether there is only one unique energy minimum with both dihedral angles near 40° , though significant deviations are observed in numerous crystal structures for molecules containing diphenyl ether substructures.²³ Energy minimizations for diphenyl ether and 2-chlorodiphenyl ether with the OPLS/CM1A force field yield optimal dihedral angles of $40 \pm 4^\circ$ in both cases.

In order to attempt to assess the difference in strain energy for the ligand in the two complexes (Figures 2 and 3), single-point OPLS/CM1A calculations were performed on the extracted conformers. The results favor the perpendicular conformer by 3.4 kcal/mol. For the clamshell conformer, the contact between two *ortho*-hydrogens is short at 2.18 Å. Optimization of the extracted structure of the clamshell conformer causes the CCOCC dihedral angles to relax to 71° and 20° , the short H–H contact lengthens to 3.31 Å, and the energy declines by 7.8 kcal/mol; the terminal phenyl ring rotates to a more perpendicular arrangement. Optimization of the extracted, perpendicular conformer changes the dihedral angles to 36° and 45° , and the energy declines by 4.4 kcal/mol. In view of the similar protein–ligand interaction energies, this analysis favors the complex in Figure 2 with the perpendicular conformer for the inhibitor. However, some motional freedom can be expected for the phenoxy group in the binding site, which is desirable for binding and response to mutational variations.^{24,25} It is also likely that different substitution patterns for the phenoxy ring can change the conformational preference. It should be noted that only the ligand strain and protein–ligand interaction energies have been considered here.

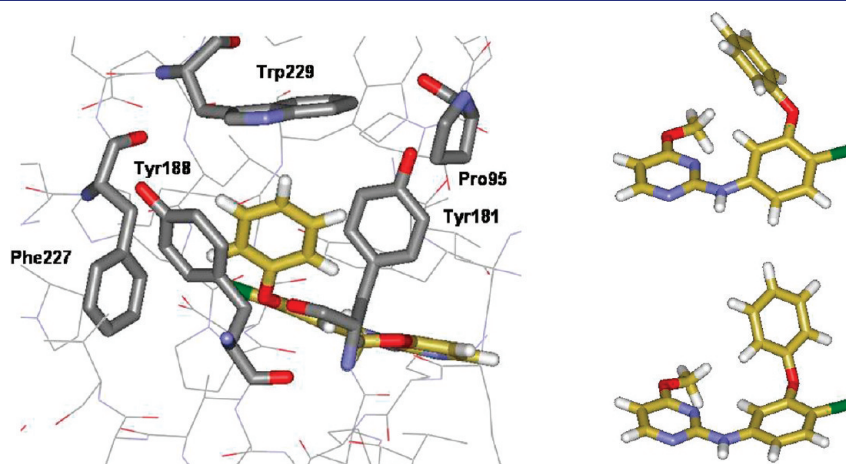
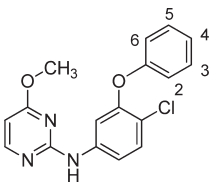


Figure 3. (Left) Alternative conformer of 3 bound to HIV-RT. (Right) Comparison of the two ligand conformations. In the top one, the faces of the phenyl rings are roughly perpendicular, while the geometry is more like a clamshell in the alternative conformer.

Table 1. FEP Results for Replacements of Chlorine and CH₃ by Hydrogen (kcal/mol)


	ΔG_{bound}	ΔG_{un}	$\Delta\Delta G_b^a$	σ^b
Cl \rightarrow H				
C2	-3.16	-2.20	-0.96	0.14
C3	1.44	1.25	0.19	0.09
C4	1.31	3.20	-1.90	0.12
C5	4.90	1.06	3.84	0.08
C6	-2.43	-1.04	-1.39	0.12
CH ₃ \rightarrow H				
C2	1.47	3.53	-2.06	0.16
C3	1.97	0.97	1.00	0.13
C4	3.16	4.01	-0.85	0.11
C5	1.70	1.29	0.42	0.14
C6	-0.79	3.77	-4.56	0.17

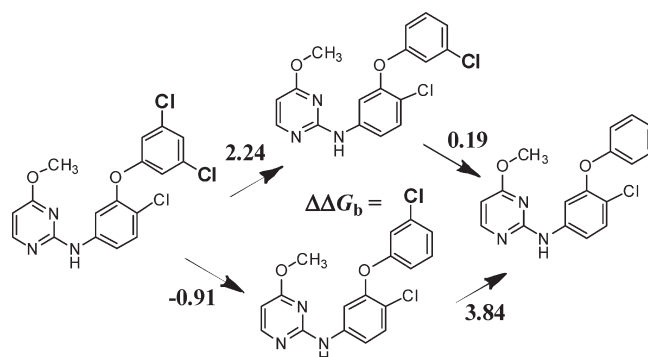
^a Computed change in free energy of binding from FEP calculations. C3 is the carbon atom in Figure 2 positioned between Tyr181 and Tyr188.

^b Statistical uncertainties computed using eq 1.

The total energies of the complexes are -3385 (perpendicular) and -3376 kcal/mol (clamshell); however, the separation is sensitive to small differences in the convergence of the optimizations.

Chlorine and Methyl Scans. Starting from **3**, placement of substituents on the phenoxy ring was considered first. FEP calculations were performed for the conversion of each hydrogen in the phenoxy ring of **3** to a chlorine or methyl group. The perpendicular conformer (Figure 2) was used as a starting point for the FEP calculations. The chloro and methyl derivatives of **3** were also built using BOMB, and each was converted to **3** in the FEP calculations. The FEP calculations include 1250 water molecules for the complexes and extensive configurational sampling, which could interconvert the ligand conformers. The FEP results are listed in Table 1, with $\Delta\Delta G_b$ representing the predicted change in free energy of binding for the chlorine- or methyl-to-hydrogen conversion. A positive value indicates that chlorine or a methyl group is preferred over hydrogen. The structure in Table 1 also corresponds to the structure in Figure 2, with the 2- and 3-positions being proximal to Y188; in the FEP calculations C2 and C6 are not equivalent, as they do not interconvert during the MC simulations. The barrier for rotation of the substituted phenoxy ring in the complexes is sufficiently high that, with normal MC sampling, these equivalent positions do not interconvert. The normal range of such dihedral angle changes for a MC move is $\pm 15^\circ$. Though larger moves could be attempted, which would allow interconversion of the equivalent positions, knowing the exact preferences at each position provides added design information.

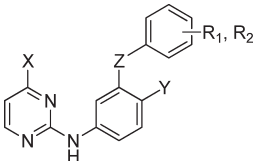
The results indicated that gains in binding should be achievable by substitutions only at C3 and C5. The preferences are not obvious by visual inspection of the built complex structures; often, one cannot tell if a nonbonded contact is attractive or somewhat too short. The convergence of the calculations for the chlorine analogues was checked using the 3,5-dichloro derivative,

**Figure 4.** Computed differences in free energies of binding, $\Delta\Delta G_b$ (kcal/mol), for chlorophenyl analogues. The hysteresis of 0.50 kcal/mol for the cycle provides a measure of the precision of the calculations.

as summarized in Figure 4. The hysteresis for the cycle of four FEP calculations, 0.50 kcal/mol, was consistent with the individual uncertainties in Table 1. The results also indicated that 3, 5-disubstitution was viable. During the MC simulations for the complexes, the conformation of the ligand did not convert from perpendicular to clamshell. In the simulations for the isolated ligands in water, display of numerous configurations also did not reveal any evidence for sampling of clamshell conformers. The dominant conformation is perpendicular, with the methyl group of the methoxy substituent packed well against the phenoxy ring.

As summarized in Table 2, the 2-, 3-, and 4-methyl analogues, **6**–**8**, were prepared and confirmed the preference for the 3-methyl compound; **7** provided a significant activity gain to 0.54 μM , compared to **3** at 2.5 μM . Results for **4** are included to demonstrate the benefits of the methoxy group in **3**. The 3-Cl and 3,5-dichloro analogues, **9** and **10**, were then prepared. Though they are also more potent than **3**, greater activity gains might have been expected on the basis of the results in Table 1. An issue for the activities is that the computed results are for free energies of binding and the EC_{50} is for a cell-based assay. It may be noted that the correlation between observed cell-based and enzymatic activities for NNRTIs is high, with r^2 values of 0.7–0.9.²⁷ The FEP results normally provide valuable qualitative guidance, while quantitative accord with the cell assay results is not expected.⁵ For example, chlorine has a higher Hansch π value (0.71) than a methyl group (0.56) or hydrogen (0.0),²⁶ so addition of chlorine to a phenyl ring is expected to make a molecule more lipophilic than addition of a methyl group. The more lipophilic compound may then partition more into cell membranes and also be lost to nonspecific complexation with other cellular proteins. Another small point is that the computed results have not been corrected for possible symmetry effects. For example, the parent **3** and the 3,5-dichloro analogue **10** have a factor of 2 advantage for binding over the unsymmetrical **9**, if there is strong preference for **9** binding with the chlorine in just the 3-position or the 5-position.

Continuing, a Cl-to-CN change in the anilinyloxy ring of **9** did provide an expected^{6b} boost to 0.64 μM for **11**. On the basis of the EC_{50} values for **9**–**11**, ca. 0.4 μM might have been anticipated for the 3,5-dichloro analogue **12**, but this was masked by the sudden enhancement of the cytotoxicity to 0.27 μM . The 3, 5-dimethyl analogue **13** was also prepared and yielded an EC_{50} of 0.49 μM , but it too was somewhat cytotoxic, with a CC_{50} of 1.3 μM . The sensitivity of the CC_{50} to structural changes is often high, as demonstrated here for **11** and **12** and considered further

Table 2. WT Inhibitory Activity (EC₅₀) and Cytotoxicity (CC₅₀) in μ M for Pyrimidines with HIV-1


compd	X	Y	Z	R ₁ ^a	R ₂	EC ₅₀ ^b	CC ₅₀ ^c
3	OCH ₃	Cl	O	—	—	2.5	38
4	H	Cl	O	—	—	13.0	30
5	OCH ₃	H	O	3-Cl	—	9.1	33
6	OCH ₃	Cl	O	2-CH ₃	—	NA	13
7	OCH ₃	Cl	O	3-CH ₃	—	0.54	18
8	OCH ₃	Cl	O	4-CH ₃	—	10	>100
9	OCH ₃	Cl	O	3-Cl	—	1.1	23
10	OCH ₃	Cl	O	3-Cl	5-Cl	0.80	4.3
11	OCH ₃	CN	O	3-Cl	—	0.64	>100
12	OCH ₃	CN	O	3-Cl	5-Cl	NA	0.27
13	OCH ₃	CN	O	3-CH ₃	5-CH ₃	0.49	1.3
14	OCH ₃	CN	O	3-CN	—	0.31	8.5
15	OCH ₃	CN	O	3-CV	—	0.26	6.9
16	CH ₃ CH ₂	CN	O	3-CV	—	0.048	0.36
17	SCH ₃	CN	O	3-CV	—	0.048	1.2
18	CH(CH ₃) ₂	CN	O	3-CV	—	0.046	4.1
19	c-C ₃ H ₅	CN	O	3-CV	—	0.032	1.1
20	c-C ₃ H ₅	CN	O	3-CV	5-Cl	0.012	1.1
21	c-C ₃ H ₅	CN	O	3-CV	5-F	0.0085	0.26
22	c-C ₃ H ₅	CN	O	3-F	5-F	0.78	4.3
23	c-C ₃ H ₅	CN	O	3-Cl	5-CN	0.015	0.15
24	c-C ₃ H ₅	CN	O	3-CIV	—	0.49	1.9
25	OCH ₃	Cl	S	—	—	0.32	21
26	OCH ₃	Cl	S	3-Cl	—	0.31	4.9
27	OCH ₃	Cl	S	3-CH ₃	—	0.31	8.9
28	OCH ₃	CN	S	3-Cl	—	0.091	0.29
29	OCH ₃	CN	S	3-CH ₃	—	0.062	0.47
30	c-C ₃ H ₅	CN	S	—	—	NA	0.039
d4T						1.4	>100
nevirapine						0.11	>100
efavirenz						0.002	15
etravirine						0.001	11
rilpivirine ^d						0.0004	8

^a CV = E-cyanovinyl. CIV = E-chlorovinyl. ^b For 50% protection in MT-2 cells; antiviral curves used triplicate samples at each concentration. NA for EC₅₀ > CC₅₀. ^c For 50% inhibition of MT-2 cell growth; toxicity curves also used triplicate samples. ^d Reference 7.

below. The origin of the cytotoxicity is unclear, but it is expected to arise from multiple mechanisms. In any event, it is desirable to have a safety margin (CC₅₀/EC₅₀) of ca. 1000 or more in the WT assay, as in the cases of the approved drugs in Table 2. The optimization strategy has been to drive down the EC₅₀ values to the low nM range and hopefully achieve CC₅₀ values at μ M levels.

Phenoxy versus Thiophenyl. An excursion at this point was to consider replacing the oxygen linker with sulfur, which might insert the terminal phenyl ring farther into the π box. Thus, FEP calculations were executed for the interconversion of **3** and **25**;

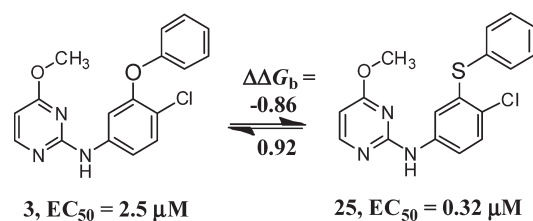


Figure 5. Computed differences in free energies of binding, $\Delta\Delta G_b$ (kcal/mol), with HIV-RT and observed anti-HIV activities for phenoxy and thiophenoxy analogues. The FEP calculations were run in both directions, yielding the indicated results in kcal/mol.

the outcome is summarized in Figure 5. The calculations were performed in both directions and consistently found that the sulfur analogue should be better bound to WT HIV-RT by 0.9 kcal/mol. Compound **25** was synthesized, and the assay results yielded a good activity gain to 0.32 μ M. It was natural to then prepare the 3-Cl and 3-CH₃ analogues with both chlorine and CN at the 4-position in the aniliny ring. The assay results for **26**–**29** were curious in that activity boosts were not found for **26** and **27**, while for the CN analogues nice EC₅₀ gains were obtained to 91 and 62 nM for **28** and **29**, respectively. However, cytotoxicity again intervened, with CC₅₀ values near 0.4 μ M. This result, coupled with the tendency of thioethers to undergo metabolic oxidation, dampened interest in pursuing them further. Later, one additional pyrimidinylthioether, **30**, which differs from **25** by Cl for CN and OCH₃ for cyclopropyl replacements, was synthesized and found to be highly cytotoxic, with a CC₅₀ of 39 nM.

Cyanovinyl Introduction and OCH₃ Replacement. So far, **11** was the best phenoxy compound, though its gain in activity over **3** was modest. However, it was clear that two chlorines could fit at the 3- and 5-positions of the phenoxy ring. This knowledge and extensive viewing of structures of **3** bound to HIV-RT, as in Figure 2, proposed something bolder. The hydrogen on C3 in the phenoxy ring is pointing directly between Tyr181 and Tyr188. Though unprecedented in NNRTI design, this suggested that it might be possible to thread a substituent, no wider than chlorine, between the two tyrosine rings. A thin, relatively rigid substituent seemed advisable, and cyanovinyl (CV) came to mind. Structure building with BOMB, followed by energy minimization, showed that complexes with compounds such as **15** should be possible with no significant protein–ligand strain. A computed structure for a complex illustrating the possible positioning of the CV group is provided in Figure 6. The CV extension is seen to fill the space well between Tyr181, Tyr188, and Trp229. It also fills the space much better in this region for the Y181C variant (Figure 6, right) than for **1** or **2**.

However, given the discussion of alternative conformations above, it was prudent to attempt again to explore alternative structures. In fact, conjugate gradient optimizations for complexes with the cyanovinyl analogue of **3** revealed four possible placements for the CV group, corresponding to attachment at either *meta* position in both the perpendicular and clamshell conformations (Figure 7). For the perpendicular conformer, it is possible for the CV group to project between Tyr181 and Tyr188 as in Figure 6, and it is also possible to place it between Pro95 and Pro97 (Figure 7, top). For the clamshell conformation, the CV group can project between Tyr188 and Phe227 or below Pro95 (Figure 7, bottom). The options shown in Figure 7B,D differ primarily in the conformation of the CV group, i.e., the dihedral angle about the bond to the phenoxy ring. The computed

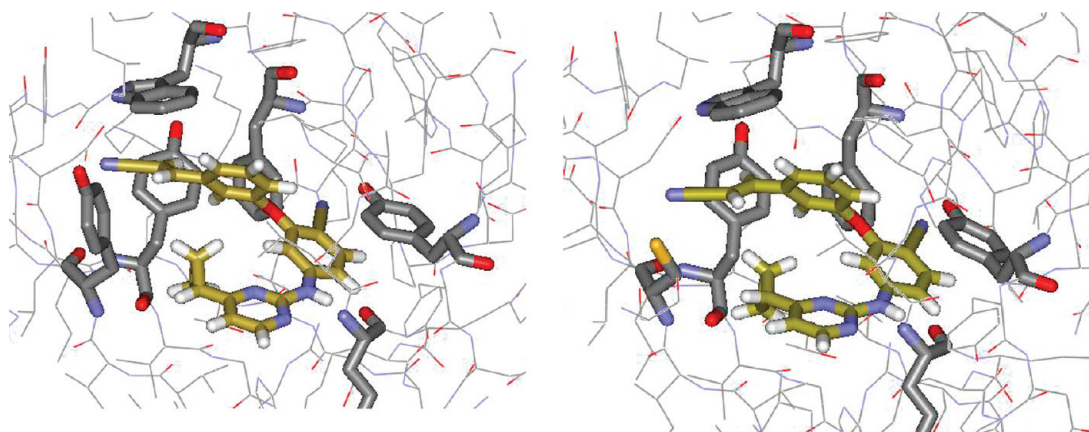


Figure 6. Optimized structures for **19** bound to wild-type (left) HIV-RT and the Tyr181Cys mutant (right). Highlighted residues are labeled in Figure 1.

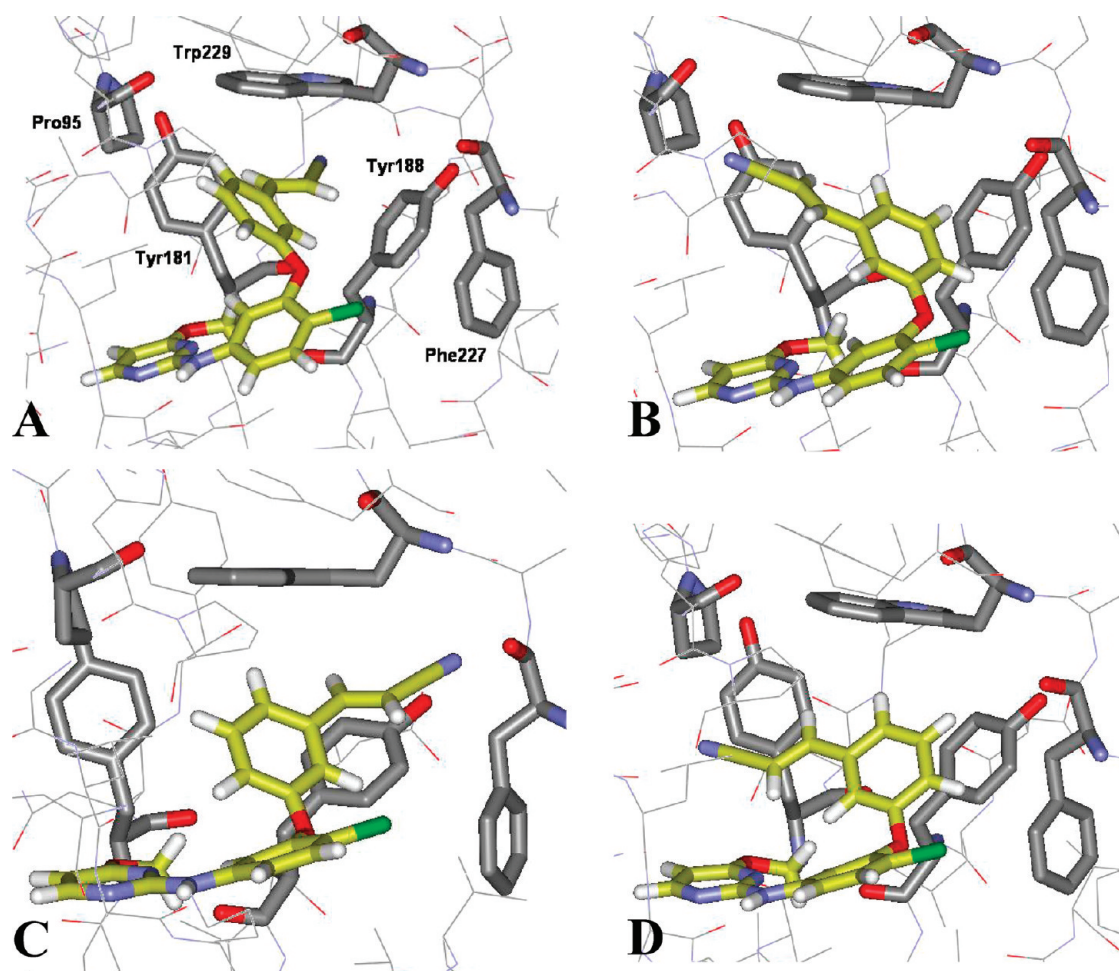
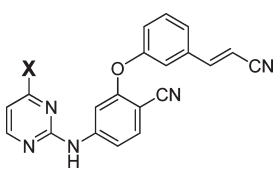


Figure 7. Computed structures illustrating alternative placement of the cyanovinyl group for analogues of **15** bound to wild-type HIV-RT: projecting (A) between Tyr181 and Tyr188; (B) toward Pro95 and Pro97; (C) between Tyr188 and Phe227; and (D) below Pro95.

protein–ligand interaction energies are again similar, -68.5 , -73.5 , -69.8 , and -72.6 kcal/mol for the structures in Figure 7A–D, respectively. The corresponding relative energies for the extracted ligands are 0.0, 0.9, 4.3, and 2.8 kcal/mol, and the total energies are -3394 , -3381 , -3382 , and -3394 kcal/mol. Thus, there is uncertainty as to the preferred conformer with a single

CV group on the phenoxy ring. However, addition of a second *meta* substituent would disfavor the conformer in Figure 7B owing to steric conflict with Tyr188.

Given the likelihood that a CV group could be accommodated, **15** was synthesized. It was found to improve the EC_{50} to $0.26\ \mu\text{M}$ for WT HIV-1 (Table 2). With this success, attention turned to

Table 3. FEP and Energy Minimization Results for Side-Chain Variations (kcal/mol)


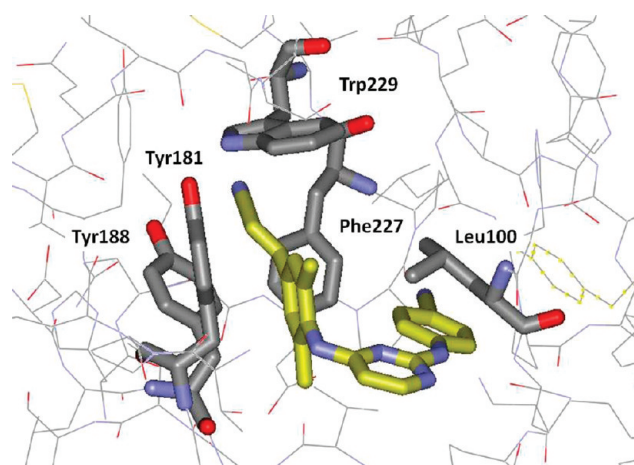
X	$\Delta\Delta G_b^a$	σ^b	E_{P-L}^c	X	$\Delta\Delta G_b^a$	σ^b	E_{P-L}^c
H	0.67	0.07	-67.6	OCF ₃	-4.52	0.40	-71.7
F	0	0	-68.1	<i>c</i> -C ₃ H ₅	-4.74	0.47	-75.6
CH ₃	-0.36	0.12	-70.8	SCH ₃	-4.96	0.43	-71.9
CH ₂ CH ₃	-2.68	0.19	-73.4	SCHF ₂	-6.16	0.44	-72.5
OCH ₃	-3.00	0.39	-69.9	CH(CH ₃) ₂	-6.55	0.23	-74.9
OCHF ₂	-4.46	0.40	-71.5				

^a Computed change in free energy of binding from FEP calculations in water relative to X = F for WT HIV-RT. ^b Statistical uncertainties computed using eq 1. ^c Protein–inhibitor interaction energy from energy minimization of the complex in vacuum with $\epsilon = 2.0$.

substitution of the pyrimidine ring. The methoxy group had been inherited from **1**; however, the change from ODMA to the cyanovinylphenoxy group is so large that it seemed likely that there might be more optimal substituents to fill the space near the C β 's of Tyr181 and Tyr188. Consequently, FEP calculations were executed to optimize the substituent on the pyrimidine ring in **15**. The calculations used the conformation of the inhibitors with the CV group pointing between Tyr181 and Tyr188. The results are summarized in Table 3, with the fluorine-substituted case as the reference point. It was very encouraging to find multiple possibilities that were predicted to yield better binding than the methoxy analogue. Among the options in Table 3, the ethyl, methylthio, cyclopropyl, and isopropyl analogues, **16**–**19**, were synthesized and assayed. They are indeed much more active than **15**, with the cyclopropyl analogue **19** being the most potent at 32 nM (Table 2; Figure 6). The qualitative accord between the EC₅₀ values and the FEP results is not perfect, perhaps owing to the conformational uncertainty; however, the FEP results indicated that there were better alternatives than methoxy and provided the motivation to pursue this course. The payoff was a factor of 8 activity boost in progressing from **15** to **19**. For comparison, Table 3 also contains the computed protein–inhibitor interaction energies, E_{P-L} , from energy minimizations in a vacuum. In this case, the E_{P-L} values correlate well with the observed activities, with ethyl and methylthio similarly better than methoxy, and with isopropyl and cyclopropyl better still.

The next step was to add again a halogen at the other *meta* position in the phenoxy ring giving the chloro and fluoro analogues, **20** and **21**; they provided further activity gains to 12 and 8.5 nM. Thus, starting with **3** or **4**, it was possible to improve the WT activity roughly 1000-fold in the course of synthesis and assaying of ca. 20 compounds. The key advances hinged on (1) the FEP results for the optimal substitution pattern of the phenoxy ring, (2) FEP guidance on the substituent in the pyrimidine ring, and (3) the recognition from the visualization and modeling that a cyanovinyl substituent should be viable in the phenoxy ring.

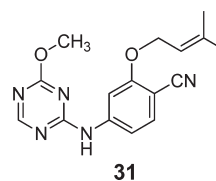
At this point, improvement in the CC₅₀ values and the activity toward the Y181C variant need to be addressed. However, first, results are noted for several additional compounds, which were synthesized to test alternative substitution patterns in the phenoxy

**Figure 8.** Depiction from the 2zd1 crystal structure²⁴ of rilpivirine bound to WT HIV-RT, illustrating the positioning of the cyanovinyl group between Tyr188 and Phe227. Carbon atoms of rilpivirine are in yellow.

ring. The EC₅₀ of 0.78 μ M for the 3,5-difluoro analogue **22** confirms the importance of the cyanovinyl group, while the 3-Cl, 5-CN analogue **23** is potent at 15 nM but too cytotoxic (CC₅₀ = 150 nM). In addition, replacing the CV group in **19** by chlorovinyl in **24** was found to cause a 15-fold activity loss. As for CV, the model building indicates that there are multiple alternatives for orientation of the chlorovinyl group in **24**, analogous to Figure 7. However, for the 3,5-disubstituted cases, **20** and **21**, the calculations favor the conformation with the CV group projecting between Tyr181 and Tyr188 or between Tyr188 and Phe227.

In closing this section, it is noted that the presence of a CV group in NNRTIs has precedent, most notably in the recently approved drug rilpivirine. However, the topology of rilpivirine is very different from that of the present NNRTIs, such that there is no option for the CV group of rilpivirine except to be positioned between Tyr188 and Phe227 (Figure 8).²⁴ For rilpivirine, the CV group is inserted into the π box from the left side near Tyr181, while it is inserted from the right side for the present CV-containing NNRTIs.

Pyrimidine versus Triazine. It was previously found that the 1,3,5-triazine **31** is more than 100-fold less cytotoxic (CC₅₀ = 42 μ M) than the analogous pyrimidine **1** (0.23 μ M).^{6c} The reduction in WT activity from 2 nM for **1** to 11 nM for **31** is comparatively small.



The 4,6-dimethoxy analogue of **31** was also potent (EC₅₀ = 22 nM) and nontoxic (CC₅₀ > 100 μ M).^{6c} Thus, it was natural to consider switching to triazines for the cyanovinylphenoxy series in order to improve the cytotoxicity from the level for **21** and hopefully from that of **20**. To gauge the potential impact on WT potency, FEP calculations were executed for the pyrimidine-to-triazine conversions with a methoxy or cyclopropyl group on the heterocycle. As summarized in Figure 9, the results were encouraging, indicating that there would be a small penalty with

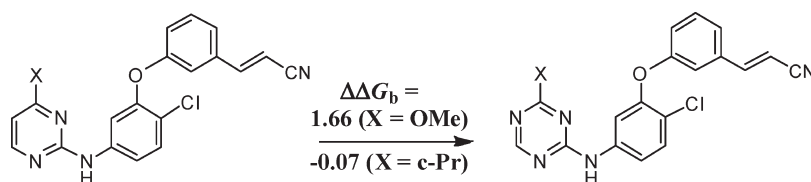
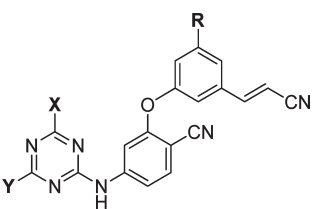


Figure 9. Computed differences in free energies of binding, $\Delta\Delta G_b$ (kcal/mol), with HIV-RT for conversion of pyrimidines to 1,3,5-triazines. The computed statistical uncertainties in both cases are ± 0.33 kcal/mol.

Table 4. Assay Results in μM for Triazines with WT HIV-1^a



compd	X	Y	R	EC ₅₀	CC ₅₀
32	OCH ₃	OCH ₃	H	0.85	6.3
33	c-C ₃ H ₅	OCH ₃	H	0.16	10
34	c-C ₃ H ₅	NH ₂	H	0.043	1.7
35	c-C ₃ H ₅	H	H	0.021	1.8
36	c-C ₃ H ₅	H	Cl	0.0025	0.12
37	c-C ₃ H ₅	H	CH ₃	0.0017	1.5

^a Details as in Table 2.

the methoxy substituent but that the cyclopropyl-containing inhibitors should have similar potency in either azine series.

Consequently, several triazine analogues were synthesized and assayed, as summarized in Table 4. The trisubstituted triazines 32–34 were prepared first owing to their relative ease of synthesis. A nice boost in potency was again found by replacing the methoxy group in 32 with cyclopropyl in 33. The greater activity of 34 (43 nM) than 33 (160 nM) is expected to stem from hydrogen-bonding of the amino group of 34 with the carboxylate group of the proximal Glu138. However, further enhanced activity is obtained by removal of the substituent at the 6-position, yielding 35 (21 nM), which is the 1,3,5-triazine analogue of the pyrimidine 19 (32 nM). Subsequent addition of the chlorine in the phenoxy ring gave the extremely potent 36 (2.5 nM), which can be compared to the pyrimidine 20 (12 nM). Thus, as anticipated by the FEP results in Figure 9, the switch to the triazine core was not deleterious for WT activity of the cyclopropyl-containing analogues.

Concerning the toxicity toward the MT-2 cells, 35 (1.8 μM) showed only slight improvement over 19, and the much greater cytotoxicity for the potent triazine 36 (0.12 μM) versus the corresponding pyrimidine 20 (1.1 μM) was very surprising. This illustrates well that the structure–activity data for cytotoxicity are complex and difficult to predict. Addition of the 5-chlorine had no effect for 19 and 20, while there is a 15- or 35-fold deficit for 35 and 36, respectively. Another example is the greater than 4-fold benefit for cyano over chlorine in the aniliny ring for 9 and 11, while the opposite ordering is found by 17-fold for 26 and 28, and by 39-fold for 2 and 1.^{6c} For the pyrimidines 12, 13, and 26–29, it appears that cytotoxicity diminishes for replacement of chlorine by a methyl group in the phenoxy ring. So, 37 was the

Table 5. Inhibitory Activity (EC₅₀) and Cytotoxicity (CC₅₀) in μM for Wild-Type and the Tyr181Cys Variant Strain of HIV-1^a

compd	WT		Y181C	
	EC ₅₀	CC ₅₀	EC ₅₀	CC ₅₀
1	0.002	0.23	NA	0.11
2	0.010	9.0	NA	11.0
17	0.048	1.2	0.25	0.98
19	0.032	1.1	0.16	0.98
20	0.012	1.1	0.032	0.82
31	0.011	42.0	12.5	20.0
35	0.021	1.8	0.25	2.2
36	0.0025	0.12	0.0049	0.073
37	0.0017	1.5	0.015	2.2
d4T	1.4	>100	0.64	>100
nevirapine	0.11	>100	NA	>100
efavirenz	0.002	15.0	0.010	>0.1
etravirine	0.001	11.0	0.008	>0.1
rilpivirine	0.0004 ^b	8.0 ^b	0.0013 ^b	

^a See footnotes in Table 2. ^b From ref 7, using MT4 cells.

final compound to be prepared. The idea paid off. 37 is a very potent NNRTI (1.7 nM), and with a CC₅₀ of 1.5 μM , it has a safety margin of about 1000.

Viral Mutations. The remaining issue is the performance of the designs incorporating the 3-cyanovinylphenoxy group on the troublesome Tyr181Cys-containing variant form of HIV-1. The strategy was to reduce contact with Tyr181 and to better fill the space that is vacated by the Tyr181-to-Cys change. The present NNRTIs also incorporate several rotatable bonds, which is viewed as beneficial for responding to structural changes in the binding site.^{24,25} The results are summarized for some of the more potent compounds in Table 5, which includes reference data for five drugs.

As noted above, 1 and 2 show no activity against the Y181C strain, though the CC₅₀ for 1 is low (100–200 nM), which would mask any activity above that level. The triazine 31 corresponding to 1 does show weak antiviral activity toward the Y181C variant (12.5 μM). When new NNRTIs were obtained with EC₅₀ values below 100 nM in the WT assay, the mutant assay was initiated. The first Y181C results for the thiomethylpyrimidine 17 and the cyclopropyl analogue 19 were very encouraging, with EC₅₀ values of 250 and 160 nM. Addition of the 5-Cl group in 20 achieved a significant milestone, with EC₅₀ values below 50 nM toward both the WT virus and the Y181C variant. The cyclopropylpyrimidine 35 was found to perform similarly to its pyridine analogue 19, while 6-fold gains in potency were obtained with 36

over **20** for both the WT virus and the Y181C variant. The resultant EC₅₀ values for **36** of 2.5 nM (WT) and 4.9 nM (Y181C) are striking, given the starting point of the original phenoxy compound **3**. In addition, the fold-change (ratio of Y181C to WT activities) of only a factor of 2 for **36** and its greater potency toward the Y181C variant than for the reference NNRTIs, efavirenz and etravirine, are notable. Finally, the potency results for the methyl analogue **37** are also excellent, with EC₅₀ values of 1.7 and 15 nM toward the WT and mutant viruses, which are similar to those for efavirenz and etravirine. The CC₅₀ values for **37** are also good, at 2 μ M. The improved performance of the 3,5-disubstituted compounds, **20**, **36**, and **37**, can be attributed to more complete filling of space in the region spanning between Cys181, Pro95, and Pro97.

CONCLUSION

The present study demonstrates the benefit of extensive molecular modeling for efficient discovery of enzyme inhibitors. The calculations featured structure building with the molecule growing program BOMB and free energy perturbation calculations for estimation of relative free energies of binding. The key goal was to obtain antiviral agents with high potency toward variant forms of HIV-1 that incorporate the clinically important Tyr181Cys mutation in HIV reverse transcriptase. With guidance from the computations, it was possible to progress from the parent phenoxy-containing **3** with micromolar activity to the extremely potent analogues **36** and **37** with low-nanomolar potency against both wild-type HIV-1 and the Tyr181Cys variant. The transformation only required the synthesis and assaying of roughly 30 compounds. The FEP calculations were essential for predicting optimal substitution patterns for the phenoxy and pyrimidinyl rings of **3** and for investigating the change of the heterocycle from pyrimidine to triazine. A key outcome is the structurally novel NNRTI **37**, which has both high potency and a large safety margin.

An issue that emerged is the need for better understanding of the origins and structure–activity relationships for the T-cell cytotoxicity, which provided sudden roadblocks at several points, e.g., for **21**, **28**, and **36**. The extreme cytotoxicity of the structurally simple compound **30** is particularly intriguing. Interesting complexity also arose concerning the preferred conformations of the new NNRTIs when bound to HIV-RT, as illustrated in Figures 3 and 7. Ongoing computational and experimental investigations are addressing further these structural questions and activity toward additional viral variants.

ASSOCIATED CONTENT

S Supporting Information. Synthetic details; NMR and HRMS spectral data for the compounds in Tables 2 and 4; complete refs 7 and 11. This material is available free of charge via the Internet at <http://pubs.acs.org>.

AUTHOR INFORMATION

Corresponding Author

karen.anderson@yale.edu; william.jorgensen@yale.edu

ACKNOWLEDGMENT

Gratitude is expressed to the National Institutes of Health (AI44616, GM32136, GM49551) for support and to Dr. Julian Tirado-Rives for computational assistance. Receipt of the following

reagents through the NIH AIDS Research and Reference Reagent Program, Division of AIDS, NIAID, NIH, is also greatly appreciated: MT-2 cells, catalog no. 237, and nevirapine-resistant HIV-1 (N119), catalog no. 1392, from Dr. Douglas Richman; HTLV-III_B/H9, no. 398, from Dr. Robert Gallo; and HIV-1_{IIIB} (A17 variant) from Dr. Emilio Emini.

REFERENCES

- (1) (a) Prajapati, D. G.; Ramajayam, R.; Yadav, M. R.; Giridhar, R. *Bioorg. Med. Chem.* **2009**, *17*, 5744–5762. (b) de Bethune, M.-P. *Antiviral Res.* **2010**, *85*, 75–90.
- (2) (a) Kohlstaedt, L. A.; Wang, J.; Friedman, J. M.; Rice, P. A.; Steitz, T. A. *Science* **1992**, *256*, 1783–1790. (b) Smerdon, S. J.; Jäger, J.; Wang, J.; Kohlstaedt, L. A.; Chirino, A. J.; Friedman, J. M.; Rice, P. A.; Steitz, T. A. *Proc. Natl. Acad. Sci. U.S.A.* **1994**, *91*, 3911–3915.
- (3) (a) Rossotti, R.; Rusconi, S. *HIV Therapy* **2009**, *3*, 63–77. (b) Chiao, S. K.; Romero, D. L.; Johnson, D. E. *Curr. Opin. Drug Disc. Dev.* **2009**, *12*, 53–60. (c) Adams, J.; Patel, N.; Mankaryous, N.; Tadros, M.; Miller, C. D. *Ann. Pharmacotherapy* **2010**, *44*, 157–165.
- (4) Richman, D. D.; Margolis, D. M.; Delaney, M.; Greene, W. C.; Hazuda, D.; Pomerantz, R. J. *Science* **2009**, *323*, 1304–1307.
- (5) Jorgensen, W. L. *Acc. Chem. Res.* **2009**, *42*, 724–733.
- (6) For example, see: (a) Jorgensen, W. L.; Ruiz-Caro, J.; Tirado-Rives, J.; Basavapathruni, A.; Anderson, K. S.; Hamilton, A. D. *Bioorg. Med. Chem. Lett.* **2006**, *16*, 663–667. (b) Ruiz-Caro, J.; Basavapathruni, A.; Kim, J. T.; Wang, L.; Bailey, C. M.; Anderson, K. S.; Hamilton, A. D.; Jorgensen, W. L. *Bioorg. Med. Chem. Lett.* **2006**, *16*, 668–671. (c) Thakur, V. V.; Kim, J. T.; Hamilton, A. D.; Bailey, C. M.; Domaoal, R. A.; Wang, L.; Anderson, K. S.; Jorgensen, W. L. *Bioorg. Med. Chem. Lett.* **2006**, *16*, 5664–5667. (d) Kim, J. T.; Hamilton, A. D.; Bailey, C. M.; Domaoal, R. A.; Wang, L.; Anderson, K. S.; Jorgensen, W. L. *J. Am. Chem. Soc.* **2006**, *128*, 15372–15373. (e) Zeevaert, J. G.; Wang, L.; Thakur, V. V.; Leung, C. S.; Tirado-Rives, J.; Bailey, C. M.; Domaoal, R. A.; Anderson, K. S.; Jorgensen, W. L. *J. Am. Chem. Soc.* **2008**, *130*, 9492–9499. (f) Leung, C. S.; Zeevaert, J. G.; Domaoal, R. A.; Bollini, M.; Thakur, V. V.; Spasov, K.; Anderson, K. S.; Jorgensen, W. L. *Bioorg. Med. Chem. Lett.* **2010**, *20*, 2485–2488.
- (7) Janssen, P. A. J.; et al. *J. Med. Chem.* **2005**, *48*, 1901–1919.
- (8) (a) Jorgensen, W. L.; Tirado-Rives, J. *J. Comput. Chem.* **2005**, *26*, 1689–1700. (b) Jorgensen, W. L.; Maxwell, D. S.; Tirado-Rives, J. *J. Am. Chem. Soc.* **1996**, *118*, 11225–11236. (c) Jorgensen, W. L.; Tirado-Rives, J. *Proc. Natl. Acad. Sci. U.S.A.* **2005**, *102*, 6665–6670. (d) Jorgensen, W. L.; Chandrasekhar, J.; Madura, J. D.; Impey, R. W.; Klein, M. L. *J. Chem. Phys.* **1983**, *79*, 926–935.
- (9) Jorgensen, W. L.; Ravimohan, C. *J. Chem. Phys.* **1985**, *83*, 3050–3054.
- (10) For recent reviews, see: (a) Chipot, C.; Pohorille, A. In *Free Energy Calculations: Theory and Applications in Chemistry and Biology*; Chipot, C., Pohorille, A., Eds.; Springer Series in Chemical Physics 86; Springer-Verlag: Berlin, 2007; pp 33–75. (b) Jorgensen, W. L.; Thomas, L. T. *J. Chem. Theory Comput.* **2008**, *4*, 869–876. (c) Michel, J.; Essex, J. W. *J. Comput. Aided Mol. Des.* **2010**, *24*, 639–658.
- (11) Das, K.; et al. *J. Med. Chem.* **2004**, *47*, 2550–2560.
- (12) Lu, N.; Kofke, D. A.; Woolf, T. B. *J. Comput. Chem.* **2004**, *25*, 28–39.
- (13) Allen, M. P.; Tildesley, D. J. *Computer Simulations of Liquids*; Clarendon: Oxford, 1987.
- (14) Purstinger, G.; De Palma, A. M.; Zimmerhofer, G.; Huber, S.; Ladurner, S.; Neyts, J. *Bioorg. Med. Chem. Lett.* **2008**, *18*, 5123–5125.
- (15) Maiti, D.; Buchwald, S. L. *J. Am. Chem. Soc.* **2009**, *131*, 17423–17429.
- (16) Gong, D.; Li, J.; Yuan, C. *Synth. Commun.* **2005**, *35*, 55–66.
- (17) Reyes-Gutiérrez, P. E.; Camacho, J. R.; Ramírez-Apan, M. T.; Osornio, Y. M.; Martínez, R. *Org. Biomol. Chem.* **2010**, *8*, 4374–4382.
- (18) (a) Popovic, M.; Read-Connole, E.; Gallo, R. C. *Lancet* **1984**, *2*, 1472–1473. (b) Popovic, M.; Sarngadharan, M. G.; Read, E.; Gallo, R. C. *Science* **1984**, *224*, 497–500.

- (19) (a) Haertle, T.; Carrera, C. J.; Wasson, D. B.; Sowers, L. C.; Richmann, D. D.; Carson, D. A. *J. Biol. Chem.* **1988**, *263*, 5870–5875. (b) Harada, S.; Koyanagi, Y.; Yamamoto, N. *Science* **1985**, *229*, 563–566.
- (20) Lin, T. S.; Luo, M. Z.; Liu, M. C.; Pai, S. B.; Dutschman, G. E.; Cheng, Y. C. *Biochem. Pharmacol.* **1994**, *47*, 171–174.
- (21) Ray, A. S.; Yang, Z.; Chu, C. K.; Anderson, K. S. *Antimicrob. Agents Chemother.* **2002**, *46*, 887–891.
- (22) Richman, D.; Shih, C.-K.; Lowy, I.; Rose, J.; Prodanovic, P.; Goff, S.; Griffin, J. *Proc. Natl. Acad. Sci. U.S.A.* **1991**, *88*, 11241–11245.
- (23) (a) Hao, M.-H.; Haq, O.; Muegge, I. *J. Chem. Inf. Model.* **2007**, *47*, 2242–2252. (b) Brameld, K. A.; Kuhn, B.; Reuter, D. C.; Stahl, M. *J. Chem. Inf. Model.* **2008**, *48*, 1–24.
- (24) Das, K.; Bauman, J. D.; Clark, A. D., Jr.; Frenkel, Y. V.; Lewi, P. J.; Shatkin, A. J.; Hughes, S. H.; Arnold, E. *Proc. Natl. Acad. Sci. U.S.A.* **2008**, *105*, 1466–1471.
- (25) Wang, D.-P.; Rizzo, R. C.; Tirado-Rives, J.; Jorgensen, W. L. *Bioorg. Med. Chem. Lett.* **2001**, *11*, 2799–2802.
- (26) Hansch, C.; Leo, L.; Unger, S. H.; Kim, K. H.; Nikaitani, D.; Lien, E. J. *J. Med. Chem.* **1973**, *16*, 1207–1216.
- (27) Rizzo, R. C.; Udier-Blagovic, M.; Wang, D. P.; Watkins, E. K.; Kroeger Smith, M. B.; Smith, R. H., Jr.; Tirado-Rives, J.; Jorgensen, W. L. *J. Med. Chem.* **2002**, *45*, 2970–2987.